Monthly Notices of the ROYAL ASTRONOMICAL SOCIETY

Mon. Not. R. Astron. Soc. **406,** 230–236 (2010) doi:10.1111/j.1365-2966.2010.16693.x

The evolutionary sequence of submillimetre galaxies: from diffuse discs to massive compact ellipticals?

E. Ricciardelli,[1,2]★ I. Trujillo,[1,2] F. Buitrago[3] and C. J. Conselice[3]

[1]*Instituto de Astrofísica de Canarias, Vía Lactea s/n, E-38200 La Laguna, Tenerife, Spain*
[2]*Departamento de Astrofísica, Universidad de La Laguna, E-38205 Tenerife, Spain*
[3]*School of Physics and Astronomy, University of Nottingham, Nottingham NG7 2RD*

Accepted 2010 March 15. Received 2010 March 15; in original form 2009 October 15

ABSTRACT

The population of compact massive galaxies observed at $z > 1$ is hypothesized, both observationally and in simulations, to be merger remnants of gas-rich disc galaxies. To probe such a scenario, we analyse a sample of 12 gas-rich and active star-forming submillimetre galaxies (SMGs) at $1.8 < z < 3$. We present a structural and size measurement analysis for all of these objects using very deep Advanced Camera for Surveys (ACS) and Near Infrared Camera and Multi-Object Spectrometer (NICMOS) imaging in the Great Observatories Origins Deep Survey (GOODS) North field. Our analysis reveals a heterogeneous mix of morphologies and sizes. We find that four galaxies (33 ± 17 per cent) show clear signs of mergers or interactions, which we classify as early-stage mergers. The remaining galaxies are divided into two categories: five of them (42 ± 18 per cent) are diffuse and regular disc-like objects, while three (25 ± 14 per cent) are very compact, spheroidal systems. We argue that these three categories can be accommodated into an evolutionary sequence, showing the transformation from isolated, gas-rich discs with typical sizes of 2–3 kpc, into compact ($\lesssim$1 kpc) galaxies through violent major merger events, compatible with the scenario depicted by theoretical models. Our findings that some SMGs are already dense and compact provide strong support to the idea that SMGs are the precursors of the compact, massive galaxies found at slightly lower redshift.

Key words: galaxies: active – galaxies: evolution – galaxies: high-redshift – galaxies: starburst – submillimetre: galaxies.

1 INTRODUCTION

Observations have shown that massive spheroids at high redshift are remarkably smaller than their local counterparts (e.g. Daddi et al. 2005; Trujillo et al. 2006a, 2007; Longhetti et al. 2007; Buitrago et al. 2008; Cimatti et al. 2008; van Dokkum et al. 2008). This population of galaxies must evolve into local massive ellipticals based on their stellar masses; however, it is not yet clear what the primary mechanism is which increases their sizes by a factor of 4 to match the local galaxy population. Although various effects (i.e. dry major mergers, observational biases, selection effects; see e.g. Valentinuzzi et al. 2010) may explain the observed size evolution of these systems, a physically motivated favoured mechanism is the growth in size by later minor mergers with less dense galaxies (Bournaud, Jog & Combes 2007; Naab, Johansson & Ostriker 2009; Hopkins et al. 2009a). This scenario has the advantage, in that it facilities the growth in galaxy sizes while permitting a mild evolution in velocity dispersion as observed (e.g. Cappellari et al. 2009; Cenarro & Trujillo 2009).

An additional problem is understanding how these objects were first formed. An emerging picture (e.g. Hopkins et al. 2007; Cimatti et al. 2008; Hopkins et al. 2009b) for the formation of these compact systems predicts that massive, gas-rich galaxies at very high redshift become unstable following a major merger event, triggering a short-lived starburst within ∼0.1 Gyr. Theoretical models (Khochfar & Silk 2006; Hopkins et al. 2007) have shown that the size of the remnant strongly depends upon the degree of dissipation involved, being very small in the case of strongly dissipative mergers. Since at high redshift ($z \gtrsim 2$) galaxies are more gas-rich than they are today (Erb et al. 2006), the degree of dissipation is expected to be high and the resulting remnant extremely compact, with sizes $\lesssim$1 kpc.

Given the great amount of gas involved in these star formation processes, we expect the progenitors of massive compact galaxies to be undergoing a high amount of star formation, and hence should be detectable in the submillimetre (sub-mm; Narayanan et al. 2010). To test this hypothesis, we examine in this paper a sample of sub-mm galaxies (SMGs), which have been imaged with *Hubble Space Telescope* (*HST*) in deep exposures, to probe their structural properties. SMGs are among the most luminous ($L \simeq 10^{13}\,L_{\odot}$) and rapidly star-forming [star formation rate (SFR) $\simeq 10^3\,M_{\odot}\,yr^{-1}$]

★E-mail: elenaricci@iac.es

galaxies in the high-redshift Universe (Hughes et al. 1998; Eales et al. 2000; Smail et al. 2002; Coppin et al. 2006; Tacconi et al. 2006, 2008; Menéndez-Delmestre et al. 2009), and are believed to be the precursors of local early-type galaxies (Swinbank et al. 2006). As their local counterparts, the ultraluminous infrared galaxies, the origin for their high fluxes is thought to be a strong starburst and/or active galactic nuclei (AGN) activity, likely triggered by a major merger (Clements et al. 1996; Murphy et al. 1996; Sanders & Mirabel 1996). It is also plausible that many SMGs are similar to the hyperluminous infrared galaxies (HLIRGs, $L_{\rm IR} > 10^{13}\,{\rm L}_{\odot}$; Rowan-Robinson 2000), containing a similar amount of molecular gas and an extreme SFR (Farrah et al. 2002a,b).

Furthermore, the similarity between the stellar mass surface densities of SMGs and the compact massive galaxies at lower redshifts (Tacconi et al. 2006, 2008; Cimatti et al. 2008) makes SMGs natural candidates for being the precursors of these compact galaxies. This paper tests this hypothesis and investigates whether the proposed theoretical scenario for the formation of massive compact galaxies is compatible with present deep imaging and star formation analysis of these sub-mm systems. To explore this, we probe the sizes of the SMGs in various phases, which we construct based on morphology and structure, and test whether the SFRs of these galaxies are in agreement with theoretical expectations. Secondly, we probe whether the different observed morphologies of the SMGs can be fitted into the evolutionary sequence proposed by current massive galaxies formation models.

This paper is structured as follows. In Section 2, we describe our sample. In Section 3, we explain the method adopted for our analysis. In Section 4, we present our results and discuss their implication in Section 5. Throughout, we assume the following cosmology: $H_0 = 70\ {\rm km\,s^{-1}\,Mpc^{-1}}$, $\Omega_{\rm m} = 0.3$ and $\Omega_\Lambda = 0.7$, and we use *AB* magnitudes.

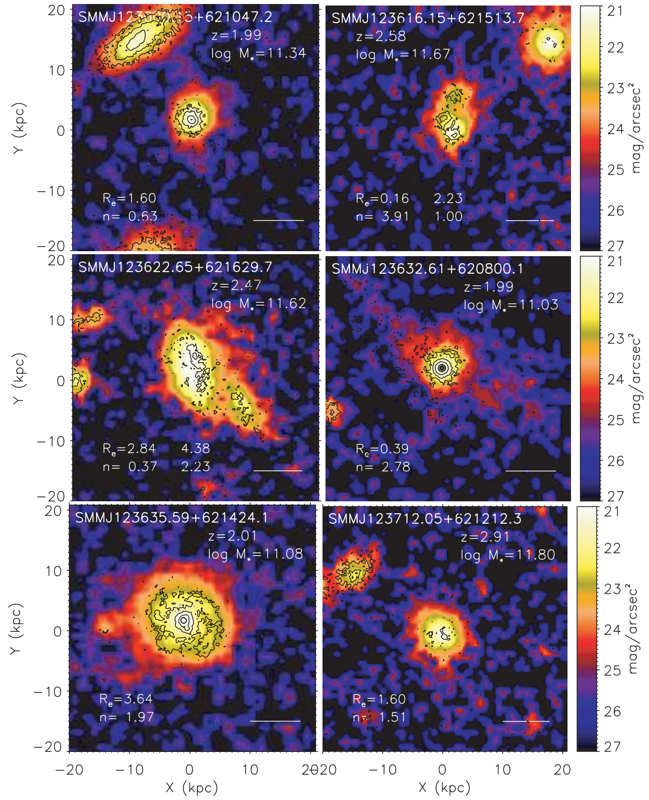

Figure 1. NICMOS images of our sample of SMGs with ACS contours overlapped. Contour levels of 24,23,22,21 and 20 mag arcsec^{-2} are shown with increasing thickness. For each galaxy, we indicate redshift, logarithmic stellar mass (in units of solar masses), effective radius (in kpc) and Sérsic index. The white line in the lower-right corner is 1 arcsec in size.

2 DATA

Our target selection is based on the following criteria, needed to characterize the nature of our high-redshift SMGs: (i) very deep images [particularly with Advanced Camera for Surveys (ACS) on the *HST*] to detect signatures of interactions; (ii) systems within and similar to the redshift range where the massive compact galaxies have been detected (i.e. $2 \lesssim z \lesssim 3$), ideally based on spectroscopic redshifts; (iii) our SMGs should be massive ($M > 10^{11}\,{\rm M}_{\odot}$) to ensure that these objects are indeed the progenitors of the lower redshift massive galaxy population.

For the above reasons, the number of SMGs that we can explore is limited. We adopt as our parent sample the SMGs from Michałowski, Hjorth & Watson (2009). This paper contains spectroscopic redshifts (from Chapman et al. 2005), multiwavelength photometric data points collected from the literature, including *Spitzer* observations. This allows for the determination of accurate SFRs and stellar masses for 76 massive SMGs (see Michałowski et al. 2009 for these values and the details in how they were calculated). The resulting range of stellar mass is quite small: 10^{11}–$10^{12}\,{\rm M}_{\odot}$. For these reasons, this sample of SMGs is the progenitor of a fraction of local massive ellipticals, as well as the compact galaxies at high redshift. Since we are interested in the high-redshift population, we restrict our analysis to the redshift range: $1.8 < z < 3$. The original stellar masses from this catalogue are converted from a Salpeter initial mass function (IMF) to a Kroupa IMF (Kroupa 2001).

Our new analysis is based on deep archival *HST* ACS and NICMOS images of these sources, where we find images for 12 sources in the GOODS-North field. We also investigated sources in other fields (e.g. Webb et al. 2003; Clements et al. 2004), but these have too shallow observations to be useful for our purposes.[1]

Our final collection of images is as follows: we have ACS images in the F850LP filter (z band) for all 12 objects, and NICMOS Camera 3 (NIC-3) data from the GOODS NICMOS Survey (Bluck et al. 2009; Conselice et al., in preparation) in the F160W filter (*H* band) for six objects. The z-band data, at 5 orbits depth, reaching a magnitude limit of $z = 27$ mag (15σ), have been drizzled to a scale of 0.03 arcsec with a point spread function (PSF) Full Width at Half-Maximum of 0.1 arcsec. The NICMOS images, at 3 orbits depth (limiting magnitude of $H = 26.8$ mag, 5σ), were combined to produce images with a pixel scale of 0.1 arcsec and PSF size of 0.3 arcsec. Note that at $z \sim 2.5$ the ACS data trace the near-ultraviolet (NUV) rest frame, whereas the NICMOS imaging shows the *B*-band rest frame. The NICMOS and ACS images of the final sample are shown in Figs 1 and 2, respectively.

All the objects in our sample show hints of AGN activity either from optical spectral features or from X-ray and radio detections. However, it is unlikely that these AGN dominate the bolometric emissivity in such objects. The reason for this is that all the spectral energy distributions are well fit by pure star-forming models, without the need of an AGN contribution (Michałowski et al. 2009). The mid-infrared (IR) spectra of these SMGs further confirm that they

[1]These observations typically have integration times <7000 s compared to the >27 000 s for the GOODS-N imaging.

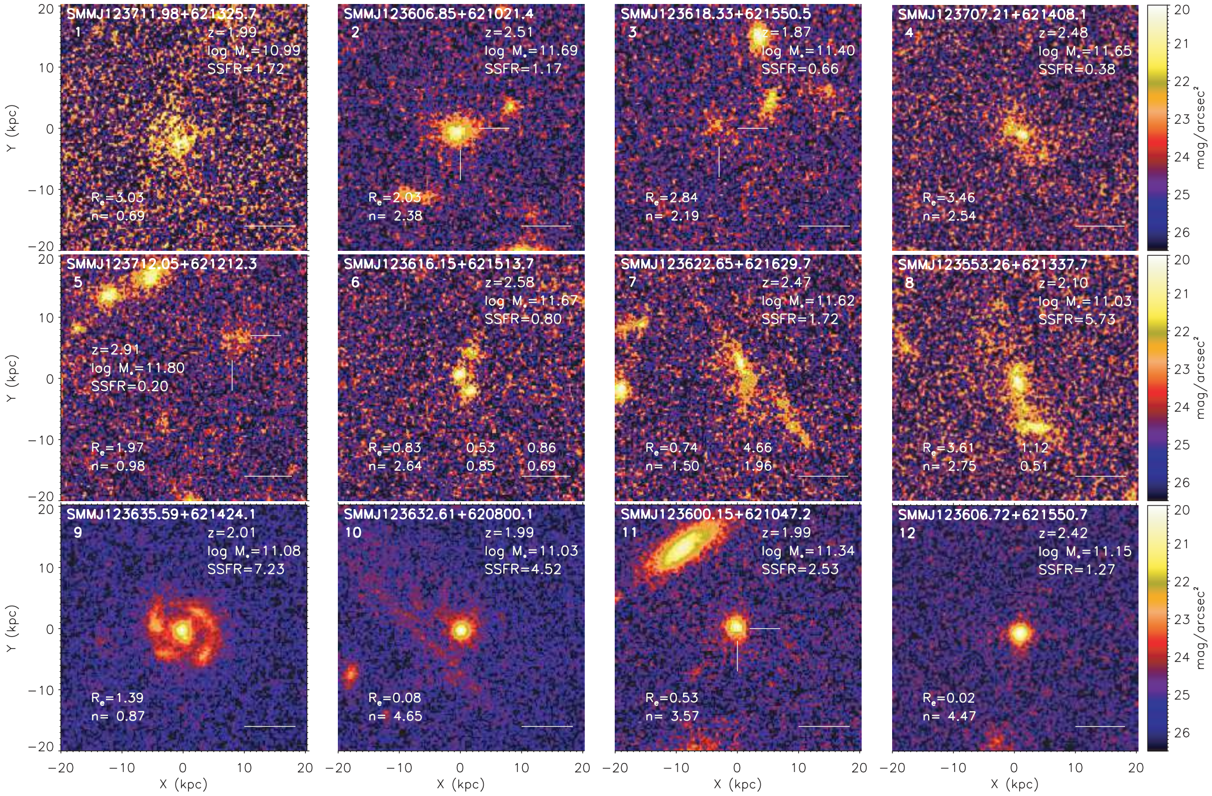

Figure 2. ACS images of our sample of 12 SMGs. The galaxies are ordered according to the evolutionary sequence described in Section 4. The first five, from left to right and top to bottom, are the disc-like objects, the next four are the ongoing mergers, and the final three are our classified compact systems. Each panel shows a box size of 40 × 40 kpc. The white line in the lower-right corner shows the 1 arcsec scalelength. In the cases where the target object is not obvious, it is indicated by two white bars. As in Fig. 1 stellar masses are in units of solar masses and effective radii in units of kpc. SSFRs are in Gyr^{-1}.

are starburst dominated without a bolometrically significant AGN (Pope et al. 2008). Moreover, as shown by Alexander et al. (2005), the X-ray to far-IR luminosity ratio is much lower than that found in quasi-stellar objects, indicating that the contribution of the AGN to the total luminosity cannot be higher than 10 per cent. More recently, Laird et al. (2010) found that the X-ray emission in SMG is largely due to star formation activity and, even in the cases where the presence of AGN is confirmed, it is not the dominant contributor to the bolometric luminosity, except in rare cases. Therefore, we expect that the properties of our sub-mm selected galaxies are not biased by AGN activity.

3 ANALYSIS

Morphological parameters and sizes are measured on our sample through the two-dimensional fitting code GALFIT (Peng et al. 2002). We model the light distribution of the sources with a Sérsic profile, deriving the Sérsic index n, the axis ratio b/a and the semimajor effective radius r_e in arcsec. We scale the radius to the physical scale in kpc relative to the redshift of the source and circularize it through $R_\mathrm{e} = r_\mathrm{e}\sqrt{b/a}$. The robustness of GALFIT in recovering sizes and structural parameters using *HST* data was assessed in several previous papers (e.g. Trujillo et al. 2006b, 2007; Cimatti et al. 2008), through the use of simulated galaxies, and is found to be robust at the resolution and depth of our *HST* imaging.

To check the reliability of our measurements against changes in the PSF shape along the images, we use up to five different natural stars, as found in our fields, as PSFs. We measure the structural parameters for each object five times, taking as our final measurement the biweight estimator, and its confidence interval as the uncertainty in the measurement. Most of the sources have an uncertainty of $\lesssim$20 per cent in the measured size and $\lesssim$30 per cent in the Sérsic index. Only two cases (SMMJ123606.72+621550.7 and SMMJ123632.61+620800.1) contain large errors based on the ACS imaging analysis, as their effective radii are close to the size of the PSF.

In the NICMOS images, the most uncertain measures are found for the compact source SMMJ123632.61+620800.1, and for the merging system SMMJ123616.15+621513.7, where the NICMOS resolution does not resolve the three components seen in the ACS observations. In most of the cases, contaminating neighbours are present in the image, and we account for these by fitting the surface brightness profile of these neighbours together with the target object. As shown by Häussler et al. (2007), the simultaneous fit allows one to recover structural parameters more reliably than deriving them using masks. Likewise, in the case of mergers, the interacting systems are fit at the same time. The results of our analysis are presented in Table 1, where size, Sérsic index and axis ratio are shown for the ACS and NICMOS data.

By comparing sizes and Sérsic indices measured in different filters, we find that the two estimates for the isolated systems agree to within 3σ. The reason for the slight differences in these fits may be ascribed to the morphological *k*-correction, where different aspects of the stellar populations for these galaxies are observed at different wavelengths. This is particularly relevant within actively star-forming galaxies or those with dust, such as the systems we examine in this paper. Note that at the median redshift of our sample ($\simeq$2.3), the NICMOS filter is probing the rest-frame optical, while

Table 1. Properties of SMGs.

Galaxy[a]	z^b	$\log \frac{M}{M_\odot}$ [c]	SSFR[d] (Gyr^{-1})	R_{AB} [e]	ACS R_e (arcsec)	ACS R_e (kpc)	ACS n	ACS b/a	NICMOS R_e (arcsec)	NICMOS R_e (kpc)	NICMOS n	NICMOS b/a	Class[f]
SMMJ123711.98+621325.7	1.992	10.99	1.72	25.8	0.36	3.03 ± 0.03	0.69 ± 0.03	0.79 ± 0.00[g]					D
SMMJ123606.85+621021.4	2.509	11.69	1.17	25.3	0.25	2.03 ± 0.04	2.38 ± 0.00	0.70 ± 0.00					D
SMMJ123618.33+621550.5	1.865	11.40	0.66	25.9	0.34	2.84 ± 0.12	2.19 ± 0.14	0.66 ± 0.12					D
SMMJ123707.21+621408.1	2.484	11.65	0.38	26.0	0.43	3.46 ± 0.39	2.54 ± 0.73	0.43 ± 0.11					D
SMMJ123712.05+621212.3	2.914	11.80	0.20	25.5	0.25	1.97 ± 0.04	0.98 ± 0.02	0.67 ± 0.00	0.21	1.60 ± 0.11	1.51 ± 0.36	0.72 ± 0.09	D
SMMJ123616.15+621513.7	2.578	11.67	0.80	25.7	0.10	0.83 ± 0.05	2.64 ± 0.76	0.74 ± 0.07	0.02	0.16 ± 0.12	3.91 ± 2.69	0.47 ± 0.43	M
					0.07	0.53 ± 0.04	0.85 ± 0.30	0.53 ± 0.05					
					0.11	0.86 ± 0.07	0.69 ± 0.13	0.66 ± 0.06	0.28	2.23 ± 0.17	1.00 ± 0.00	0.97 ± 0.05	
SMMJ123622.65+621629.7	2.466	11.62	1.72	25.4	0.09	0.74 ± 0.04	1.50 ± 0.02	0.12 ± 0.01	0.35	2.84 ± 0.07	0.37 ± 0.02	0.41 ± 0.03	M
					0.58	4.66 ± 0.43	1.96 ± 0.17	0.10 ± 0.00	0.54	4.38 ± 0.73	2.23 ± 0.04	0.35 ± 0.04	
SMMJ123553.26+621337.7	2.098	11.03	5.73	24.7	0.43	3.61 ± 0.15	2.75 ± 0.12	0.28 ± 0.00					M
					0.14	1.12 ± 0.06	0.51 ± 0.04	0.22 ± 0.00					
SMMJ123635.59+621424.1	2.005	11.08	7.23	24.2	0.17	1.39 ± 0.28	0.87 ± 0.00	0.78 ± 0.00	0.44	3.64 ± 0.12	1.97 ± 0.08	0.81 ± 0.04	M
SMMJ123632.61+620800.1	1.993	11.03	4.52	23.6	0.01	0.08 ± 0.04	4.65 ± 1.22	1.00 ± 0.00	0.05	0.39 ± 0.73	2.78 ± 3.33	0.45 ± 0.42	C
SMMJ123600.15+621047.2	1.994	11.34	2.53	25.1	0.06	0.53 ± 0.10	3.57 ± 0.66	1.00 ± 0.00	0.19	1.60 ± 0.18	0.63 ± 0.28	1.00 ± 0.00	C
SMMJ123606.72+621550.7	2.416	11.15	1.27	23.6	0.002	0.02 ± 0.02	4.47 ± 3.12	1.00 ± 0.00					C

Notes. [a]Galaxy ID, objects without ID are the subcomponents in the merging systems.
[b]Spectroscopic redshift from Chapman et al. (2005).
[c]Stellar mass from Michałowski et al. (2009) converted to a Kroupa IMF.
[d]Specific star formation rate from Michałowski et al. (2009).
[e]Magnitudes in the *R* band (*AB* system) from Chapman et al. (2005).
[f]Morphological class: D stands for disc-like objects, M for ongoing mergers and C for compact galaxies (see Section 4).
[g]Measurements with errors equal to 0.00 mean that the parameters have been fixed in the fitting procedure.

the ACS imaging matches the rest-frame NUV. Hence, the bluer ACS band is more sensitive to the clumpy distribution of the star-forming regions. Particularly in the case of 'disc'-like galaxies, the Sérsic index measured in the NUV rest frame is smaller compared to the rest-frame optical wavebands (see also Rawat, Wadadekar & De Mello 2009). However, in most of the cases the NUV and optical rest-frame morphologies agree in their ability to discriminate between disc-like ($n < 2.5$) and early-type ($n > 2.5$) galaxies.

On the other hand, for the merging systems the measurements in the NICMOS and ACS bands show significant differences. One reason for this is the lack of resolution in the NICMOS band, which does not always allow us to resolve the merging systems, such as the case of SMMJ123616.15+621513.7 where three galaxies are seen in the z-band image, but only two in the H-band image. The system SMMJ123622.65+621629.7 is a rapidly ongoing merger which is seen in the rest-frame UV as a compact, elongated galaxy with prominent tidal features, while in the NICMOS band the tides are not resolved and the effective radius is much larger. In the case of system SMMJ123635.59+621424.1, the strong disagreement is due to the fact that in the z band we observe a multicomponent system, made up of a compact bulge with a double nucleus, plus faint spiral arms on larger scales. Since the spiral arms are too faint to be fit with a single Sérsic model, we have measured the compactness of the bulge. Rather, in the NICMOS H band the multicomponent structure is not resolved, and fits to the system reveal a much more extended profile. Hence, merging systems can appear very different at different wavelengths when using images at different resolutions, and morphological k-corrections can strongly affect our measurements.

4 RESULTS

In Fig. 2, we show the ACS images of the sample, classified according to their morphological properties. We find that SMGs display a heterogeneous mix of morphologies. We divide the sample into three main categories: disc-like objects (5/12), ongoing mergers (4/12) and compact galaxies (3/12). The first class includes the majority of the sources (42 ± 18 per cent), which show quite regular and diffuse morphologies, light profiles characteristic of late-type galaxies (i.e. $n < 2.5$) and are very faint. Although we cannot rule out that some of them are interacting systems, where the companion is not detected due to its faintness at NUV wavelengths,[2] our hypothesis is that these objects are disc-like galaxies with ongoing SFR. It is important to note that for galaxies in this category, where we have NICMOS imaging, the disc-like nature is confirmed through the rest-frame optical images.

The second category, ongoing mergers (33 ± 17 per cent), are systems where two or more components are clearly visible in the ACS band. We include in this class the source SMMJ123635.59+621424.1, since a double nucleus is visible, and it is likely to be in the final stages of a merger. Most of these interacting systems display disc-like structures with a large range in sizes. This is also confirmed in NICMOS when data are available. The final class includes three (25 ± 14 per cent) very compact, isolated sources. All of these objects show a concentrated light profile,

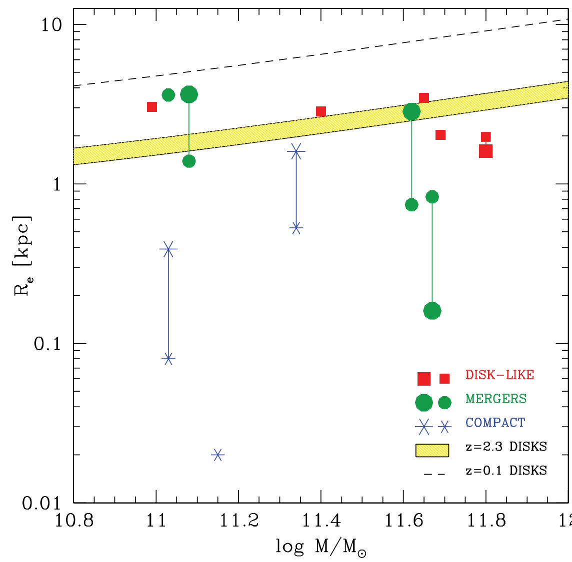

Figure 3. Stellar mass–size relation for our sample. Red squares indicate the disc-like galaxies, green circles are for the 'mergers' and blue asterisks represent the three compact objects. Large and small symbols are for NICMOS and ACS data, respectively. Overplotted is the stellar mass–size relation for disc galaxies evolved to $z = 2.3$ (yellow shaded region: upper envelope is the NICMOS-derived relation, lower envelope is the ACS-derived one), following Buitrago et al. (2008), and the local relation (black dashed line) from Shen et al. (2003).

with Sérsic indices indicative of an early-type morphology ($n > 2.5$) and $R_e \lesssim 1$ kpc. Note that the extremely small sizes measured in the ACS data (tracing the NUV) indicate that the star formation is extremely concentrated in the centre of these objects. Although the AGN contribution might play a role in shrinking the size measured in the rest-frame UV, we find that when NICMOS data are available the near-IR sizes are slightly larger but still very small compared to galaxies with similar masses in the nearby Universe.

In Fig. 3, we plot the stellar mass–size relation for our sample galaxies, divided into the three morphological classes. Overplotted is the mass–size relation for disc galaxies from Buitrago et al. (2008) at $z = 2.3$ (the median redshift of our sample):

$$R_e(M_*, z = 2.3) = \alpha(1 + z)^{-\beta} R_e(M_*, z = 0.1)\,, \qquad (1)$$

with $\alpha = 1.1$ and $\beta = 0.8$ for the NICMOS-derived sizes (upper envelope of the shaded region) and $\alpha = 1.1$ and $\beta = 1.0$ for the ACS-derived sizes (lower envelope). The local relation, $R_e(M_*, z = 0.1)$, is taken from Shen et al. (2003) based on Sloan Digital Sky Survey data. Remarkably, the sizes of the disc-like galaxies in our sample match the sizes found for the general massive galaxy population at this redshift. As the relation of Buitrago et al. (2008) does not change significantly for ACS and NICMOS data, this reinforces the idea that the ACS sizes of our disc-like objects (around 2–3 kpc) are representative of the rest-frame optical sizes of these galaxies.

We note that some of the galaxies in our sample were already studied in previous works (Chapman et al. 2003; Conselice, Chapman & Windhorst 2003; Smail et al. 2004; Almaini et al. 2005; Pope et al. 2005; Swinbank et al. 2010) using both ground-based and *HST* data. They found a higher merger fraction (≃50–60 per cent) with respect to ours (≃30 per cent), partly due to the method adopted for the classification of mergers. While the above authors use schemes based on the asymmetry parameter, in our analysis we only considered ongoing mergers, those systems where two or more distinct components are resolved in the ACS image. As mentioned

[2]Indeed two of the disc-like objects, SMMJ123711.98+621325.7 and SMMJ123707.21+621408.1, present multicomponent radio counterparts lying at the same redshift (Swinbank et al. 2004; Chapman et al. 2005). Therefore, although they appear isolated in the optical they are likely early-stage mergers (Pope et al. 2008; Tacconi et al. 2008).

above, it is also possible that dust is hiding the interacting structure and we are missing a fraction of actual mergers, hence our measured merger fraction has to be considered a lower limit.

5 DISCUSSION

Motivated by high-resolution hydrodynamical simulations (Dekel & Cox 2006; Cox et al. 2008b; Hopkins et al. 2009b; Narayanan et al. 2010), we argue that the three morphological classes outlined above could represent an evolutionary sequence, where the disc-like class represents a pre-merger phase followed by the major merger event, while the compact sources can be interpreted as the end stages of the merger, caught during or just after the coalescence. Numerical simulations naturally explain how the tidal forces involved in the interactions remove angular momentum from the systems, allowing the gas to fuel towards the centre. At this stage, the gas is compressed into a very small volume, leading to surface densities of the order of $\simeq 10^5$ M$_\odot$ pc^{-2} (Hopkins et al. 2010), close to that of molecular clouds. According to the Kennicutt law, the SFR in such conditions is extremely enhanced. Since the dynamical time-scale that drives the collapse is similar to the SFR, the system rapidly exhausts its gas while it contracts (Mihos & Hernquist 1996; Hopkins et al. 2008). Thus, it is not surprising that we observe such compact galaxies with high SFR. The models, indeed, predict a spheroidal-like morphology at the time of coalescence or just after, since the coalescence generally completes at about the same time as the gas first reaches the centre (Cox et al. 2008a).

Moreover, our findings that a fraction of the SMGs have a compact morphology agrees with measurements of the gas distribution from CO maps for many galaxies (Tacconi et al. 2006, 2008). Therefore, these compact, highly star-forming systems are likely to be in the final phase of the merger and are the transition link between starbursts and compact galaxies.

A peculiar case is represented by the system SMMJ123635.59+621424.1. We classify it as a merger event, as it appears as a double-nucleus system. However, its effective radius and Sérsic index are characteristic of those for compact galaxies. It is likely that we are measuring the compactness of the bulge component, given the faintness of the outer light. This system also shows faint signs of potential spiral structure over a scale of 5 kpc. The specific star formation rate (SSFR) of this system is the highest in our sample, compatible with being near the peak in star formation during the coalescence phase. It is worth to note that this object has the highest infrared luminosity $L = 10^{13.01}$ L$_\odot$ (from Michałowski et al. 2009) of our sample; hence, it can be considered an HLIRG, supporting the picture where HLIRGs are galaxies in their maximal star formation periods triggered by interactions.

In order to build an 'illustrative' evolutionary sequence, we can order galaxies inside a given class according to the values of their SSFR. In Fig. 4, we show as a dashed line the evolution of the SSFR in a simulated galaxy merger, taken from Narayanan et al. (2010). The simulation illustrates the evolution of the SFR in a major merger (with mass ratio 1:1) for an $\sim 2 \times 10^{13}$ M$_\odot$ dark matter halo. We have computed the SSFR taking the SFR of their fig. 1 and dividing it by the final stellar mass (8×10^{11} M$_\odot$, which is roughly the maximum stellar masses of our sample). The trend in SSFR shows a modest SFR in the pre-merger phase, in agreement with the value of our diffuse galaxies, followed by a steep rise during the starburst/merger, a peak in the coalescence phase, and then a rapid decline. The trend depicted by the simulations is matched by our data if we assume that the SSFR increases in the merging phase and then declines for the compact galaxies. The peak is reached during the coalescence,

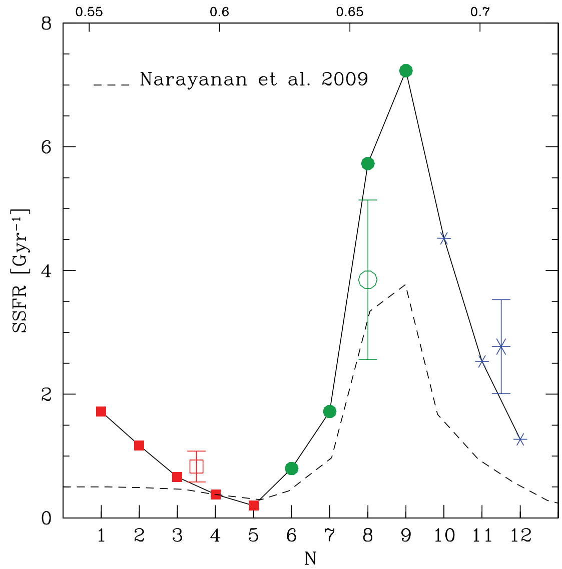

Figure 4. SSFR for our 12 SMGs (points, solid line). Different symbols refer to different morphological classes as in Fig. 3 (red squares: disc-like galaxies; green circles: mergers; blue asterisks: compact galaxies). The open symbols with error bars indicate the average SSFR for a given class. Average and standard deviations have been computed with a bootstrap resampling. The *x*-axis refers to the position of the galaxy in the proposed evolutionary sequence shown in Fig. 2. The dashed line shows the predictions of Narayanan et al. (2010) from a merger model for SMGs, with the time-scale shown in the upper axis in units of Gyr.

as it is illustrated by the source SMMJ123635.59+621424.1. In simulations, the diffuse/isolated systems are not fuelled by a new gas reservoir, as in the case for merging systems, and they simply exhaust the cold gas available. Hence, their SSFR declines with time (see Cox et al. 2008b). Therefore, in the same plot, we have indicated by the coloured points the SSFR of our sample of SMGs, with the number in the *x*-axis indicating the position in the evolutionary sequence (in Fig. 2, galaxies are ordered according to this sequence). Note that we adopt the SFR derived from the IR luminosity from Michałowski et al. (2009), using the Kennicutt (1998) relation to compute the SFR.

The fact that we can put our galaxy sample in an SSFR sequence that well matches that found in hydrodynamical simulations strengthens the conclusion that the (morphological) evolutionary sequence described above, where large diffuse systems transform themselves in compact remnants passing through a major merger event, is likely the formation mechanism for these galaxies into compact systems seen at slightly lower redshifts. Another piece of evidence supporting this theoretical merging scenario is the size of the progenitor discs we have found. Theoretically these discs are expected to have effective radius of 2–3 kpc (Dekel & Cox 2006; Hopkins et al. 2009b). This is in fact what our observations show. Given the lack of NICMOS imaging for most of the sources and the insufficient resolution in the near-IR, we were forced to use ACS imaging to constrain our morphological sequence. To better test such picture, high-sensitivity imaging in near-IR would be required, and this could be achieved only when Wide Field Camera 3 imaging will be available.

Summarizing, our data cannot reject the evolutionary picture depicted by theoretical models in which the precursors of the superdense galaxies are massive, gas-rich discs at $z \sim 2$–3, which evolve into compact remnants through dissipative major mergers.

Moreover, a cold gas accretion-driven scenario for the formation of the compact massive galaxies, as the one proposed by Dekel et al. (2009), perhaps cannot be easily supported by our data, since in this case we would likely not observe such a large diversity of size and structure for these progenitors as we observe here.

ACKNOWLEDGMENTS

We thank the referee for helpful suggestions which improved this paper. We are grateful to Philip F. Hopkins for insightful comments in relation to some theoretical issues. We also thank Karín Menéndez-Delmestre for her suggestions, and Michele Cirasuolo, Loretta Dunne and Nathan Bourne for useful discussions.

REFERENCES

Alexander D. M., Bauer F. E., Chapman S. C., Smail I., Blain A. W., Brandt W. N., Ivison R. J., 2005, ApJ, 632, 736
Almaini O., Dunlop J. S., Conselice C. J., Targett T. A., Mclure R. J., 2005, preprint (arXiv:astro-ph/0511009)
Bluck A. F. L., Conselice C. J., Bouwens R. J., Daddi E., Dickinson M., Papovich C., Yan H., 2009, MNRAS, 394, L51
Bournaud F., Jog C. J., Combes F., 2007, A&A, 476, 1179
Buitrago F., Trujillo I., Conselice C. J., Bouwens R. J., Dickinson M., Yan H., 2008, ApJ, 687, L61
Cappellari M. et al., 2009, ApJ, 704, L34
Cenarro A. J., Trujillo I., 2009, ApJ, 696, L43
Chapman S. C., Windhorst R., Odewahn S., Yan H., Conselice C., 2003, ApJ, 599, 92
Chapman S. C., Blain A. W., Smail I., Ivison R. J., 2005, ApJ, 622, 772
Cimatti A. et al., 2008, A&A, 482, 21
Clements D. et al., 2004, MNRAS, 351, 447
Clements D. L., Sutherland W. J., McMahon R. G., Saunders W., 1996, MNRAS, 279, 477
Coppin K. et al., 2006, MNRAS, 372, 1621
Cox T. J., Dutta S. N., Hopkins P. F., Hernquist L., 2008a, in Kodama T., Yamada T., Aoki K., eds, ASP Conf. Ser. Vol. 399, Panoramic Views of Galaxy Formation and Evolution. Astron. Soc. Pac., San Francisco, p. 284
Cox T. J., Jonsson P., Somerville R. S., Primack J. R., Dekel A., 2008b, MNRAS, 384, 386
Conselice C. J., Chapman S. C., Windhorst R. A., 2003, ApJ, 596, L5
Daddi E. et al., 2005, ApJ, 626, 680
Dekel A., Cox T. J., 2006, MNRAS, 370, 1445
Dekel A. et al., 2009, Nat, 457, 451
Eales S., Lilly S., Webb T., Dunne L., Gear W., Clements D., Yun M., 2000, AJ, 120, 2244
Erb D. K., Steidel C. C., Shapley A. E., Pettini M., Reddy N. A., Adelberger K. L., 2006, ApJ, 646, 107
Farrah D., Serjeant S., Efstathiou A., Rowan-Robinson M., Verma A., 2002a, MNRAS, 335, 1163
Farrah D., Verma A., Oliver S., Rowan-Robinson M., McMahon R., 2002b, MNRAS, 329, 605
Häussler B. et al., 2007, ApJS, 172, 615
Hopkins P. F., Hernquist L., Cox T. J., Robertson B., Krause E., 2007, ApJ, 669, 45
Hopkins P. F., Hernquist L., Cox T. J., Dutta S. N., Rothberg B., 2008, ApJ, 679, 156
Hopkins P. F., Bundy K., Murray N., Quataert E., Lauer T. R., Ma C.-P., 2009a, MNRAS, 398, 898
Hopkins P. F., Hernquist L., Cox T. J., Keres D., Wuyts S., 2009b, ApJ, 691, 1424
Hopkins P. F., Murray N., Quataert E., Thompson T. A., 2010, MNRAS, 401, L19
Hughes D. H. et al., 1998, Nat, 394, 241
Kennicutt R. C., Jr, 1998, ApJ, 498, 541
Khochfar S., Silk J., 2006, ApJ, 648, L21
Kroupa P., 2001, MNRAS, 322, 231
Laird E. S., Nandra K., Pope A., Scott D., 2010, MNRAS, 401, 2763
Longhetti M. et al., 2007, MNRAS, 374, 614
Menéndez-Delmestre K. et al., 2009, ApJ, 699, 667
Michałowski M. J., Hjorth J., Watson D., 2009, preprint (arXiv:0905.4499)
Mihos J. C., Hernquist L., 1996, ApJ, 464, 641
Murphy T. W., Jr, Armus L., Matthews K., Soifer B. T., Mazzarella J. M., Shupe D. L., Strauss M. A., Neugebauer G., 1996, AJ, 111, 1025
Naab T., Johansson P. H., Ostriker J. P., 2009, ApJ, 699, L178
Narayanan D., Hayward C. C., Cox T. J., Hernquist L., Jonsson P., Younger J. D., Groves B., 2010, MNRAS, 401, 1613
Peng C. Y., Ho L. C., Impey C. D., Rix H.-W., 2002, AJ, 124, 266
Pope A., Borys C., Scott D., Conselice C., Dickinson M., Mobasher B., 2005, MNRAS, 358, 149
Pope A. et al., 2008, ApJ, 675, 1171
Rawat A., Wadadekar Y., De Mello D., 2009, ApJ, 695, 1315
Sanders D. B., Mirabel I. F., 1996, ARA&A, 34, 749
Smail I., Ivison R. J., Blain A. W., Kneib J.-P., 2002, MNRAS, 331, 495
Smail I., Chapman S. C., Blain A. W., Ivison R. J., 2004, ApJ, 616, 71
Shen S., Mo H. J., White S. D. M., Blanton M. R., Kauffmann G., Voges W., Brinkmann J., Csabai I., 2003, MNRAS, 343, 978
Swinbank A. M., Smail I., Chapman S. C., Blain A. W., Ivison R. J., Keel W. C., 2004, ApJ, 617, 64
Swinbank A. M., Chapman S. C., Smail I., Lindner C., Borys C., Blain A. W., Ivison R. J., Lewis G. F., 2006, MNRAS, 371, 465
Swinbank A. M. et al., 2010, MNRAS, in press (doi:10.1111/j.1365-2966.2010.16485.x)
Rowan-Robinson M., 2000, MNRAS, 316, 885
Tacconi L. J. et al., 2006, ApJ, 640, 228
Tacconi L. J. et al., 2008, ApJ, 680, 246
Trujillo I. et al., 2006a, MNRAS, 373, L36
Trujillo I. et al., 2006b, ApJ, 650, 18
Trujillo I., Conselice C. J., Bundy K., Cooper M. C., Eisenhardt P., Ellis R. S., 2007, MNRAS, 382, 109
Valentinuzzi T. et al., 2010, ApJ, 712, 226
van Dokkum P. G. et al., 2008, ApJ, 677, L5
Webb T. M. A., Lilly S. J., Clements D. L., Eales S., Yun M., Brodwin M., Dunne L., Gear W. K., 2003, ApJ, 597, 680

This paper has been typeset from a TEX/LATEX file prepared by the author.